VOL. 16 NO. 3 1994

ISSN 0267-6605

CLINICAL MATERIALS

INCORPORATING CRITICAL REVIEWS IN BIOCOMPATIBILITY

ELSEVIER APPLIED SCIENCE

ELSEVIER

Clinical Materials 16 (1994) 127–135
1994 Elsevier Science Limited
Printed in Great Britain.
0267-6605/94/$7.00

Biomechanical Studies on Shape Effect of Hydroxyapatite Artificial Root Upon Surrounding Jawbone

Katsunari Nishihara,[a]* Masashi Nakamura[b] & Shigeru Nakagiri[c]

[a] Department of Oral Surgery, Faculty of Medicine, University of Tokyo, 7-3-1 Hongo, Bunkyo-ku, Tokyo 113, Japan
[b] Division of New Ceramics, Ashai Optical Company, 2-36-9 Maenocho, Itabashi-ku, Tokyo 174, Japan
[c] Department of Applied Physics and Applied Mechanics, Institute of Industrial Science, University of Tokyo, 7-22-1 Roppongi, Minato-ku, Toyko 106, Japan

(Received 10 September 1993; accepted 10 January 1994)

Abstract: To study the shape effect upon surrounding tissue of artificial dental root made of synthetic hydroxyapatite, this paper deals with the numerical analysis of the artificial root on functioning jawbone with the aid of the finite element method (FEM). The stress distribution around artificial roots in the shape of a cylinder, a cone, and three types of corrugated cone, including the newly tailored type implanted in the mandibular molar region, was analyzed in the plane strain state. The numerical results showed that the stress distribution was sensitive to the artificial root shape, and that the stress state was distributed in mitigatory way around the roots of the newly tailored form. The pattern of osteogenesis in the animal experiment and the finite element analysis (FEA) pattern showed a close correlation. Osteogenesis was assumed to occur in the weak or moderate stress distribution zone. The principal stress trajectory pattern in the lamina dura around the tailored artificial root was indicated as being either parallel or normal to the root surface. From this study, the biomechanical property of the tooth can be identified as a vehicle of mastication forces which disperse stresses moderately and equally upon surrounding tissues. Also, the periodontal ligament can be identified as a converting system of principal stress trajectories.

INTRODUCTION

Various kinds of dental implants made of titanium, alumina, and hydroxyapatite, which have excellent biocompatibility, have been used clinically.[1–6] At present, optimal healing around dental implants is considered to be direct, intimate contact with bone tissue, i.e. osseointegration.[2] On the other hand, development of a dental implant with functional peri-implantium and biodynamic interface has been tried.[1] Recently, some researchers have begun to invent artificial roots with functional support of collagenous peri-implantium[1,6–9] and collagenous anchoring.[10]

In this paper, results of studies on the shape effect of a newly tailored artificial root are reported. The studies were carried out with the aid of FEM and animal experiments.

The authors devised artificial roots of the fibrous tissue attachment type (new type) made of sintered hydroxyapatite with different shapes according to the implanted jaw site. Basic studies on the new type artificial root were carried out and the results were reported on the biological material effect of a newly tailored artificial root upon surrounding tissues.[7,8] The artificial root joined the jawbone with fibrous tissue resembling periodontal ligament, forming osseous structures resembling lamina dura (alveolar bone proper) around the root.[7,8] The fibrous tissues attached to the artificial

* To whom correspondence should be addressed.

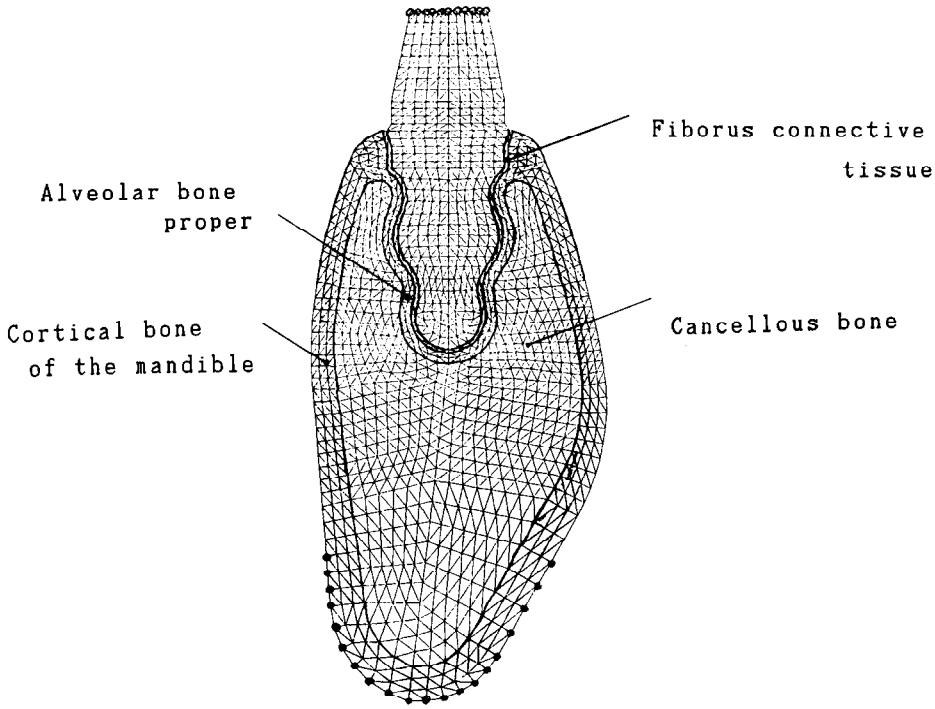

Fig. 1. Element division for FEA of new standard type artificial root.

root surface were proved to be fixed with cellularly calcified tissue resembling cementum by animal experiments using dogs.[7,8] Marked bone formation around the artificial roots in the bone marrow as well as the outer surface of the mandible was observed in undecalcified specimens from animal experiments. The pattern of newly formed bone was thought to have a close correlation to the stress distribution. Therefore, the stress distribution was analyzed in specimens in the plane strain state of a buccal–lingual section of the mandible.[9] Also, five kinds of shapes were analyzed by FEM to observe the shape effect in the same condition. After that, ankylotic (osseointegration), standard (corrugated), and cylindrical types of artificial roots were analyzed by FEM. The results were compared to those of the fibrous tissue attachment type (new type). From this study, we concluded that the stress distribution pattern in alveolar bone is influenced by root shape and loading condition to the root, and the pattern of the newly formed bone is thought to have a close correlation to the weak or moderate stress distribution zone in the finite element analysis (FEA). The trabecular bone formation around the artificial root and cortical bone formation of the mandible can be thought to coincide with the principal stress trajectories. This fact suggests that the bone remodeling system of the jaws, including alveolar bone around the roots, is in accordance with Wolff's Law.[11–17] As a result of this investigation, biomechanical properties of the tooth were found to be a vehicle of masticatory forces[9] which disperse stresses moderately and uniformly upon surrounding tissues. The periodontal ligament proved to be a converting system of principal stress trajectories.

METHOD

Initially, bone formation was compared around newly tailored artificial roots of standard type (undulated conical shape, 5 mm in diameter) in

Table 1.

Sintered compact	*Young's modulus (GPa)*	*Poisson's ratio*
Hydroxyapatite	35·2	0·28
Cortical Bone	16·1	0·45
Cancellous Bone	$5{\cdot}10 \times 10^{-1}$	0·3
Fibrous Tissue	$7{\cdot}14 \times 10^{-2}$	0·3

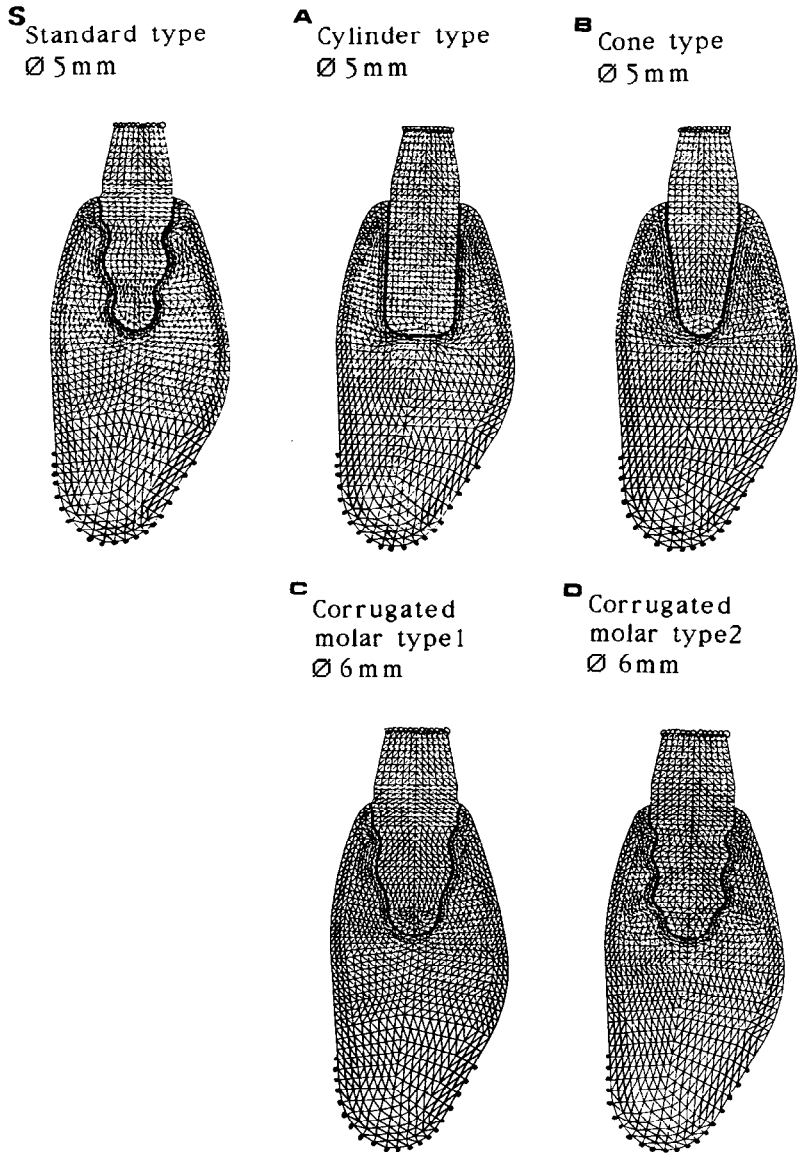

Fig. 2. Element division of five kinds of different shapes: standard types (S) of 5 mm diameter, cylinder and cone types of 5 mm diameter (A,B), and two different corrugated cone types of 6 mm diameter (C,D).

experimental specimens of dogs with the Mises' equivalent stress distribution patterns of FEA. A model of the buccal–lingual section of the mandibular premolar region was made in the plane strain state implanted with standard type artificial roots for the FEA (Fig. 1). The experimental conditions and material constants are described in Table 1.

Figure 1 shows the element division used. In this model, around the artificial root, connective tissue 0.15 mm in width and bone tissue 0.5 mm in width (alveolar bone proper) were hypothesized. A static 60 MPa load was applied to the top of the artificial roots (gray dots) with inclinations of 90°, 75°, 60°, and 45° to the horizontal plane. The fixed points were indicated as black points at the bottom of the mandible. The evaluation was performed by Mises' equivalent stress and principal stress trajectories. The results were compared to specimens of artificial roots implanted in the premolar region of the mandible in dogs. Analyses of the shape effect of the artificial roots with different forms were also carried out. Four other kinds of different shapes were analyzed, i.e. two types of 5 mm diameter (cylinder and cone shapes) and two types of 6 mm diameter (different corrugated cone shapes) (Fig. 2A–D). Loading conditions remained the same as before. Corrugated (standard) and cylindrical artificial roots of osseointegration were also analyzed and the results were compared to those of the new type artificial roots.

The amounts of stress were expressed as white,

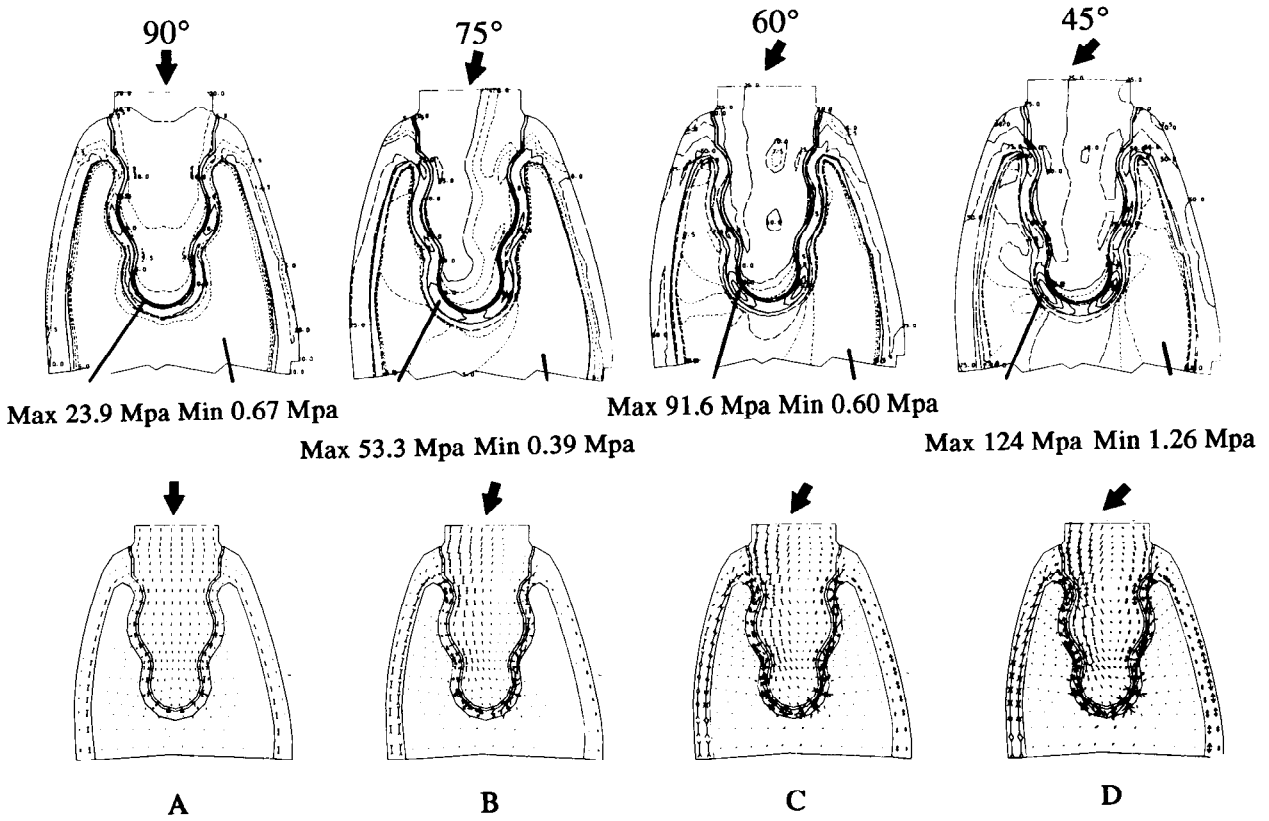

Fig. 3. FEA patterns of 5 mm tailored standard type artificial root. Upper, Mises' equivalent stress distribution patterns, and lower, principal stress trajectory patterns. Loading condition; static 6 kgf/mm loading with 90°, 75°, 60°, and 45° inclinations to horizontal plane (A–D), from left to right, respectively.

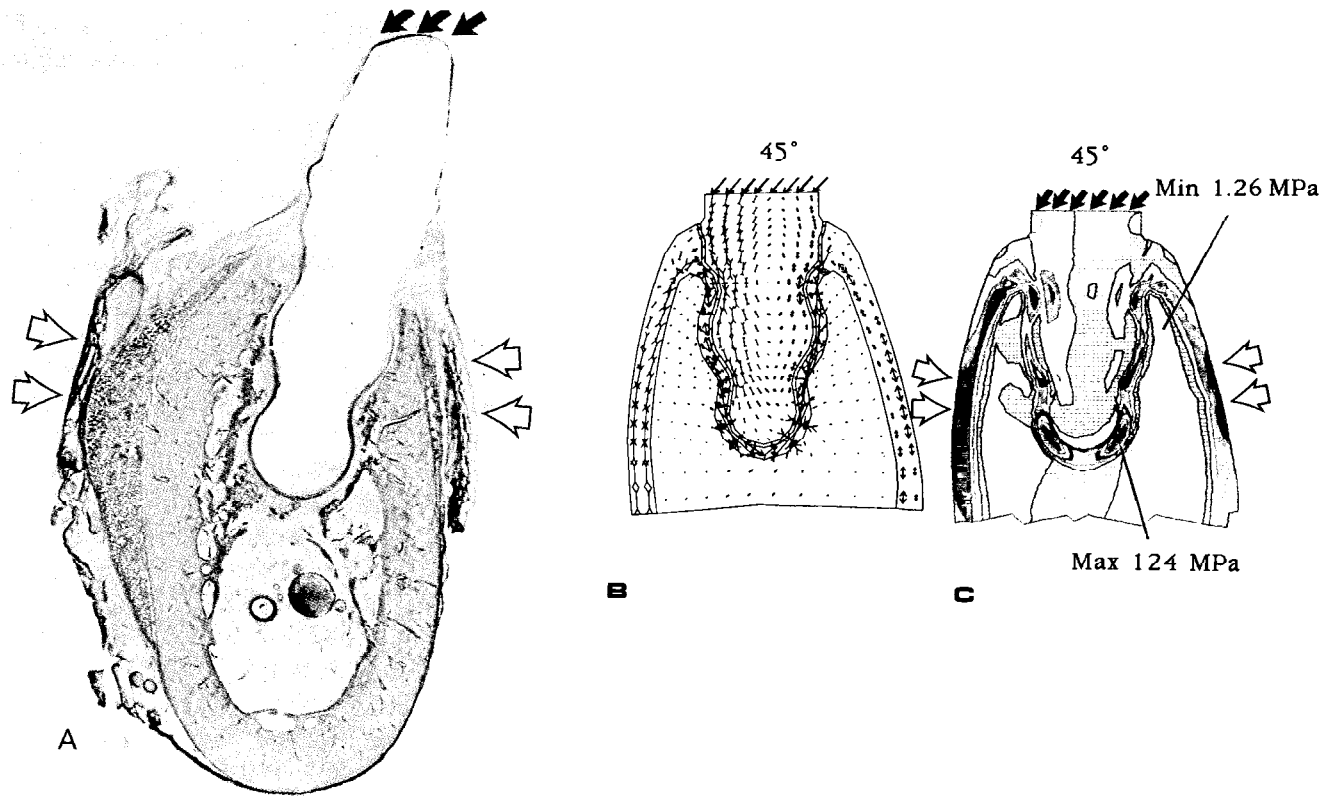

Fig. 4. Comparison of osteogenesis patterns in animal specimen and FEA of loading inclined by 45° to the horizontal plane. Specimens (A), principal stress trajectory patterns (B), and Mises' equivalent patterns (C). Osteogenesis coincides with weak and moderate stress distribution zone (A, C, arrows).

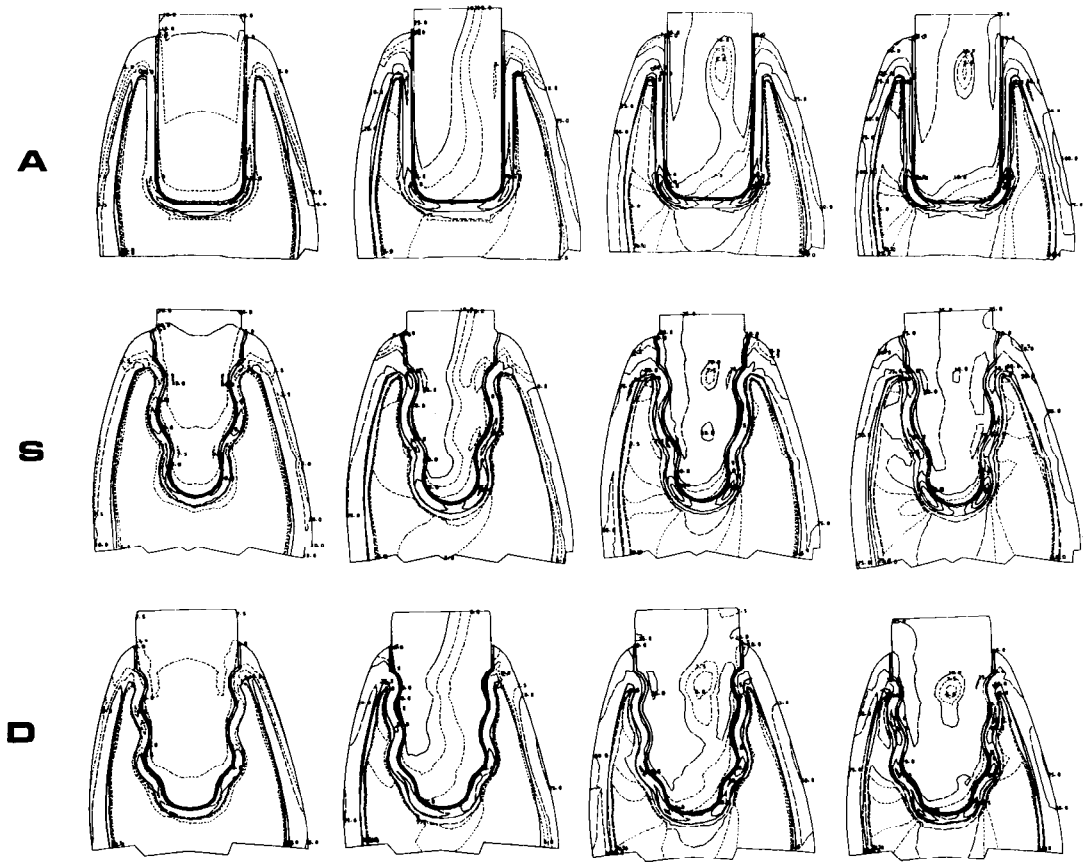

Fig. 5. Mises' equivalent stress distribution patterns of cylinder A (5 mm), standard type S (5 mm), and corrugated (6 mm) type D were compared. Loading conditions are static 6 kgf/mm with 90°, 75°, 60°, and 45° inclinations. Patterns are dependent upon shape of artificial root.

gray mesh, and gradients of gray in the order of intensity. The most condensed gray was the severe stress zone (Figs 4C and 6). The computer used was Fujitsu VP30E with software FEM4. Artificial roots used in the experiments had a cylindrical or corrugated cone columnar shape. Therefore, for an exact numerical experiment, analyses of the three-dimensional state were required. However, the aim of the analyses was not to obtain the exact stress value but the stress distribution pattern under loading conditions. Therefore, FEAs under a plane strain state were carried out. It was supposed that every part of the model was constructed of isotropic materials and within clastic limits, and neither sliding nor separating occurred at the interface of each different material with different material constants.

RESULTS

The FEA patterns of a 5 mm corrugated (standard type) artificial root are shown in Fig. 3A–D. The upper row indicates the Mises' equivalent stress distribution and the lower indicates the principal stress trajectory patterns with loading conditions of 90°, 75°, 60°, and 45° to the horizontal plane, from left to right, respectively. A comparison of the pattern of osteogenesis in the animal specimen and FEA of loading inclined by 45° to the horizontal plane is also shown (Fig. 4A–C). In the standard type of fibrous tissue attachment artificial root, the Mises' equivalent stress distribution pattern showed the values of a minimum of 1·26 MPa and a maximum of 124 MPa in mandibular bone under a loading condition of 45° to the horizontal plane. The pattern of osteogenesis in the specimen and FEA showed a close correlation (Fig. 4). The loading direction on the lower premolars of the dog in mastication was thought to be about 45° to the horizontal plane. The osteogenesis pattern was assumed to coincide with the weak or moderate stress distribution zone in the FEA pattern (Fig. 4A,C). The comparisons of Mises' equivalent stress distribution patterns of three out of the five artificial root shapes are shown in Fig. 5 under loading conditions of 90°, 75°, 60°, and 45° inclination to the horizontal plane, from left to right, respectively.

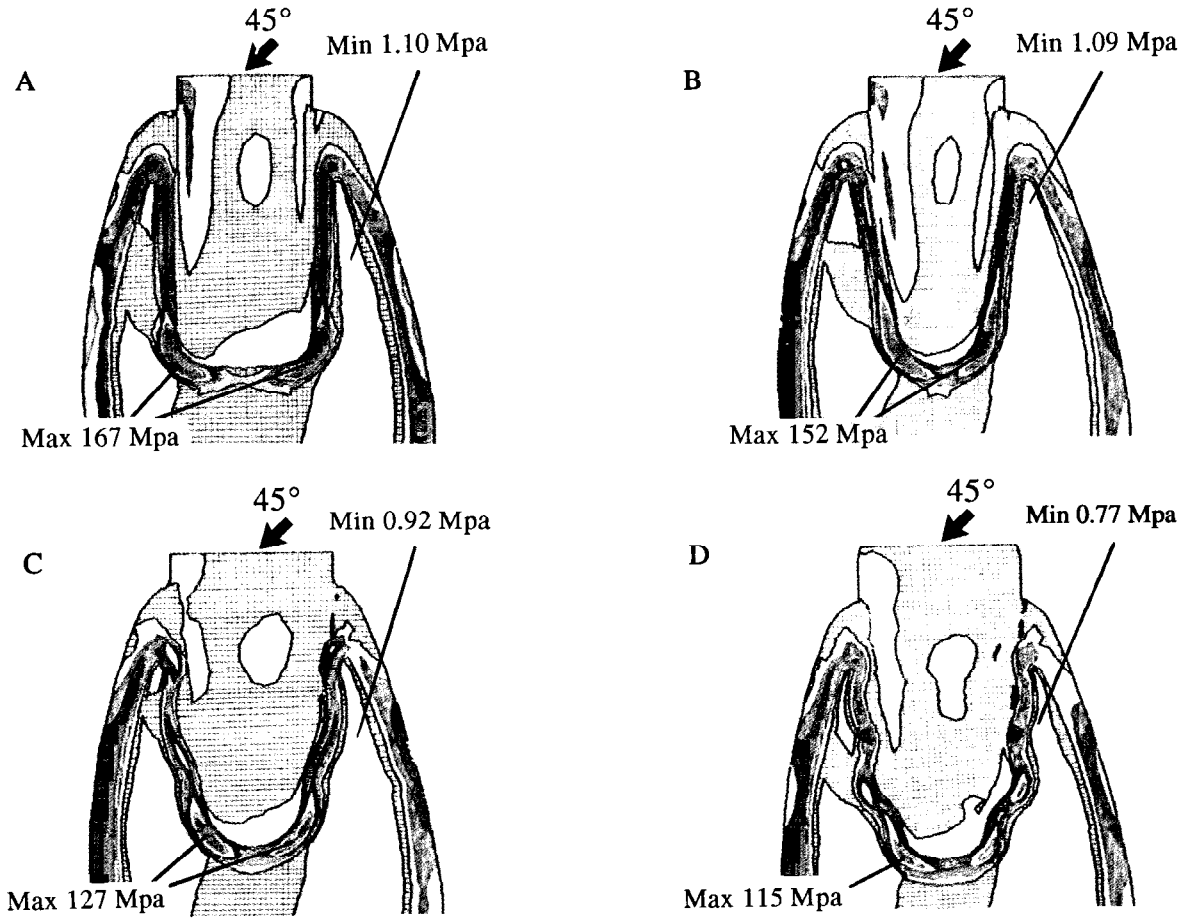

Fig. 6. A–D Mises' equivalent stress distribution patterns of cylinder A (5 mm), cone B (5 mm), corrugated C (6 mm), and corrugated molar D (6 mm) artificial roots.

From the experiment, it was ascertained that the stress distribution patterns in alveolar bone were sensitive to the artificial root shape and loading conditions to the root.

Stress distribution patterns of two 5 mm artificial roots (cylinder and cone shapes) and two 6 mm artificial roots (different corrugated shapes), with loading of 45° to the horizontal plane, are shown in Fig. 6A–D. A high stress zone could be seen at the apex and cortical regions in the cylindrical and conical types in the analysis patterns (Fig. 6A,B).

In comparison to these, smooth and moderate stress distribution patterns in the corrugated standard type artificial root could be observed (Fig. 4B). The most mitigated stress distribution pattern was observed in the 6 mm molar type of artificial root (Fig. 6D). The principal stress trajectories of a corrugated standard type artificial root (Fig. 4B) and a 5 mm cylindrical root are also shown (Fig. 7). The principal stress trajectory pattern around the standard type root was complex. In the alveolar bone proper, the stress trajectories were converted to either parallel or normal (orthogonal) to the root surface (Fig. 4B). On the other hand, in the cylindrical type, principal stress trajectories were observed parallel to the root surface except for corners of the apex in the alveolar bone proper (Fig. 7). In the case of an osseointegration (ankylotic) artificial root of corrugated standard type, the Mises' equivalent stress distribution pattern showed the values of 1.1 MPa (minimum) and 73.1 MPa (maximum) in mandibular bone under a loading direction of 45° to the horizontal plane (Fig. 8A). Principal stress trajectories could be observed continuously from the artificial root to surrounding bone in ankylotic artificial root.

DISCUSSION AND CONCLUSION

Conventionally, dental implants have been applied without a clear understanding of the biomechanical properties of the tooth. As H. Kawahara mentioned, by research in dental implantation, the

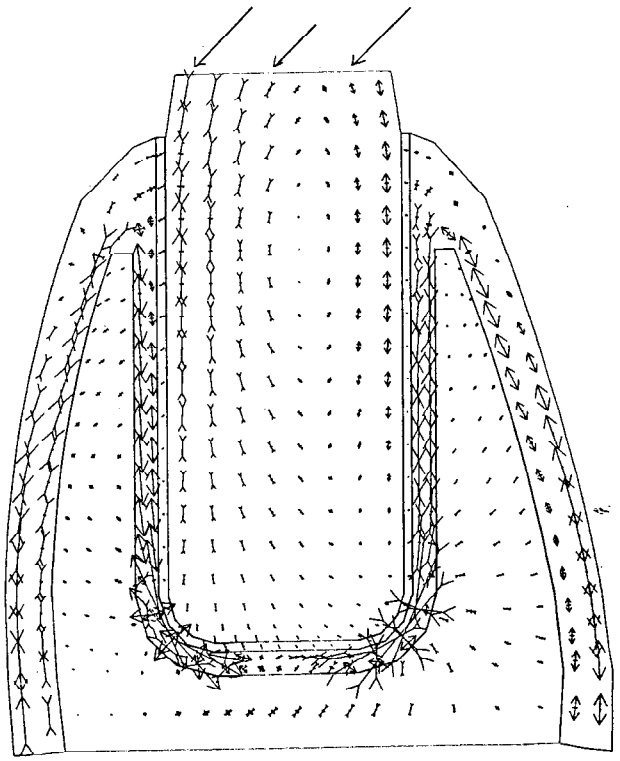

Fig. 7. Principal stress trajectory pattern of cylindrical type artificial root. Loading condition is static 6 kgf/mm with 45° inclination to horizontal plane.

question 'What is a tooth in biomechanics?' can be solved.[1] If the property of a tooth can be identified, the results can be applied to dental implants.

With the FEA, generally speaking, the stress distribution pattern is more important than the value of the stress intensity.[18] In this study, more mitigated stress distribution patterns were indicated in corrugated new type artificial roots, compared to conventional cylindrical- or conic-shaped roots in the FEA. The pattern of osteogenesis in the specimens and FEA patterns coincided, also in clinically applied cases.[9] Newly formed bone trabeculae around the artificial roots coincided with the principal stress trajectories analyzed by FEM (Figs 3, 4 and 9). The osteogenesis corresponded to the smooth or moderate stress distribution zone (Fig. 5), and the bone trabeculae around the artificial roots corresponded to the principal stress trajectories (Figs 3 and 4). Osteogenesis according to the distributed principal stress trajectories is compatible with Wolff's Law of functional form in cortical and trabecular bone formation.[11–17]

After animal experiments using dogs, the authors studied the material effect of newly tailored artificial roots of the fibrous tissue attachment type made of titanium, zirconium oxide and sintered compact

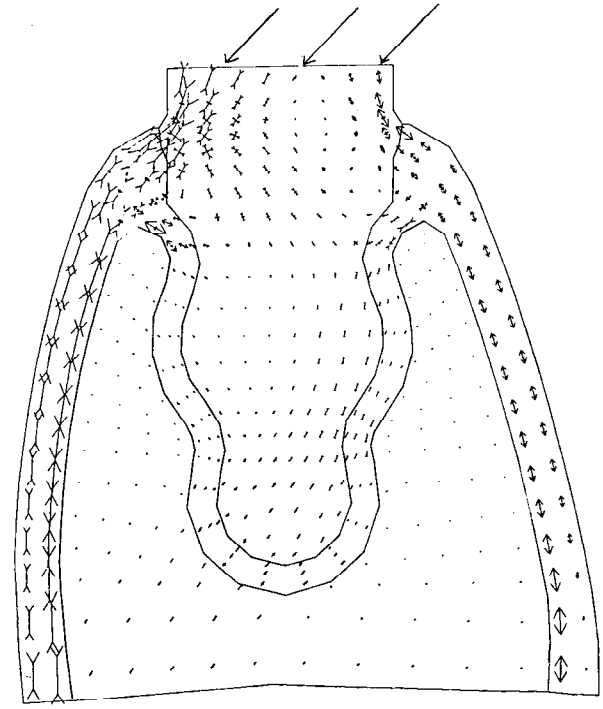

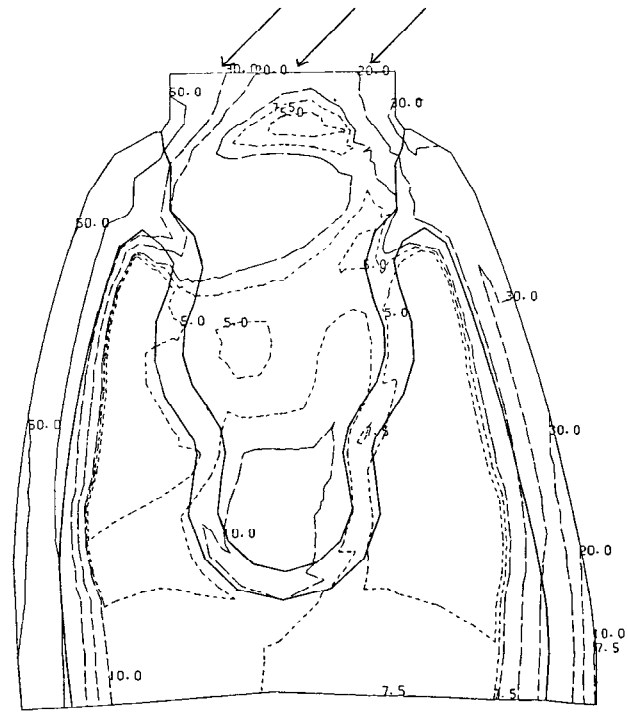

Fig. 8. Mises' equivalent stress distribution A (upper) and principal stress trajectory B (lower) patterns of ankylotic standard artificial root. Loading condition is 6 kgf/mm with 45° inclination to horizontal plane. Strong stress distribution zone along outer surfaces of cortical bone can be observed (arrows).

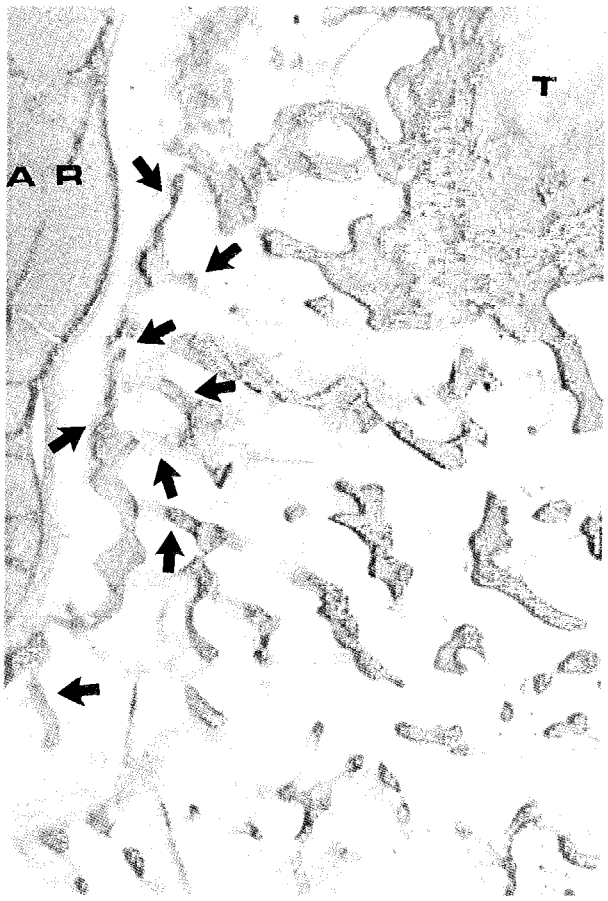

Fig. 9. Undecalcified specimen of tailored hydroxyapatite artificial root implanted in lower jaw of dog. Alveolar bond proper with trabeculae is clearly observed (arrows). Trabeculae are assumed to coincide with normal (orthogonal) principal stress trajectories to root surface exhibited in Fig. 5.
AR: artificial root, T: tooth.

hydroxyapatite and reported the results. In the experiments, fibrous tissue attachment and osteogenesis similar to alveolar bone proper were observed in all artificial roots regardless of the materials used.[7] However, among the materials observed, hydroxyapatite was unique in that calcified material resembling cementum attached to the artificial root surface.[7,8] From comparison with the FEA patterns in periodontal supportive tissues and animal experiment specimens, it was observed that the osteogenesis coincided with the analysis patterns, and the principal stress trajectories were converted by peri-implantium into orthogonal and parallel orientations according to the shape of the artificial roots. The periodontal ligament or peri-implantium (Fig. 4B) converts the trajectories of principal stress into parallel and normal orientations around the root in the alveolar bone proper. The periodontium or peri-implantium has also a shock-absorbing function with viscoelasticity of the microvascular system. Therefore, periodontal ligament or its substitute, i.e. peri-implantium, is the most important tissue for the stress transfer and absorbing system (Fig. 4B). In comparing ankylotic and fibrous tissue attachment type artificial roots in the FEA patterns, the stress distribution was shown to be different. Ankylotic roots have no stress-dispersing system; therefore, the jointing site of artificial roots in osseous tissue is disrupted or damaged under repeated severe loading because of differences in Young's modulus and Poisson's ratio. Usually, severe bone damage occurs around artificial roots in long-term functions.[1,19] From the comparison of the morphological structure of the jaw bone around the tooth with the results of the FEA of the artificial root, the following scheme for biomechanical properties of the tooth can be made (Fig. 10): the tooth is a vehicle which (1) bears multi-directed occlusal force, (2) disperses stress by its material properties and shape effect of the root, and (3) distributes it in the jawbone more moderately and almost evenly

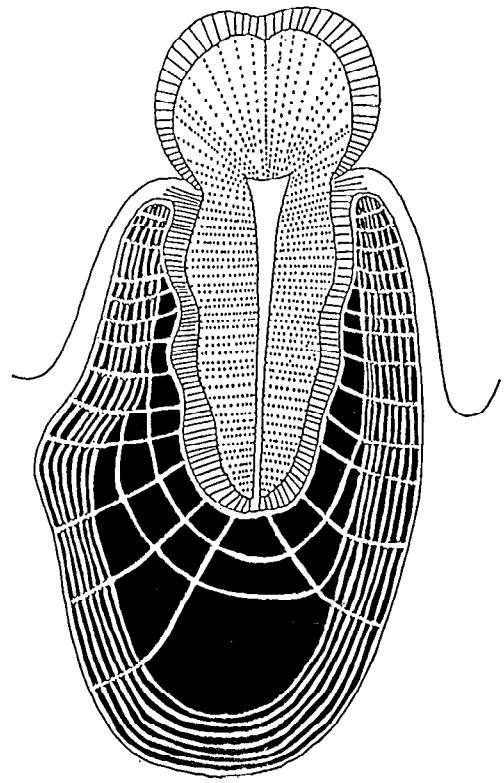

Fig. 10. Scheme explaining biomechanical property of the tooth, namely vehicle. Multi-directional occlusal force is born by vehicle of tooth, then dispersed to almost equal stresses around the root. At the periodontal ligament, principal stress trajectories are transferred to parallel and orthogonal orientation to root surface, which form alveolar bond proper and trabeculae. Contour-forming cortical bone of the jaw finally bears occlusal stresses.

in the aggregate through mastication. Namely, dispersed stresses are transferred into two components of principal stress by periodontal ligament, then transmitted into the alveolar bone proper and attached bone trabeculae. The stress trajectories are oriented continuously through the alveolar bone proper and trabeculae into the cortical bone. Finally, the cortex of the contour-forming jawbone carries the stress (Fig. 10). After all, the mammalian tooth system is a stress-carrying mechanism by contour-forming cortical bone of the jaw, not by trabeculae in the maxilla or mandible. For successful dental implantation, an understanding, not only of the biomechanical properties of the tooth and jawbone, but also of the biomechanical interactions between the tooth and jawbone is essential. As mentioned earlier, the tooth is a vehicle of masticatory force in the jawbone. Discovery of the property of the tooth in biomechanics is epoch-making in dentistry and odontology. The concept of the vehicle for mechanical characteristics of the tooth contributes to dental implant or artificial root therapeutics. Through this concept, the remodeling mechanisms, not only around the natural tooth, but also around artificial roots can be understood.

ACKNOWLEDGEMENT

This work was supported by Grant-in-aid from the Ministry of Education of Japan (05221102).

REFERENCES

1. Kawahara, H., Future vision of implantology. In *Proc. Int. Congr. Implant. and Biomater. in Stomatol. and Japan Soc. Implant Dentistry*. Ishiyaku Publishers, Tokyo, 1980, pp. 1–17.
2. Brånemark, P.-I., Osseointegration and 1st experimental background. *J. Prosthet. Dent.*, **50** (1983) 399–410.
3. Aoki, H., Kato, K. & Shiba, M., Synthesis of OH apatite by hydrothermal method, first report. *J. Dent. Apparatus Mater.*, **13** (1972) 170–6.
4. Aoki, H. & Kato, K., Synthesis of OH apatite by hydrothermal method, second report. *J. Dent. Apparatus Mater.*, **14** (1973) 36–9.
5. Aoki, H. & Kato, K., Application of apatite to dental materials, first report. *J. Dent. Apparatus Mater.*, **17** (1976) 200–5.
6. Buster, D., Warrer, K. & Karring, T., Formation of a periodontal ligament around titanium implants. *J. Periodont.*, **61**(9) (1990) 597–601.
7. Nishihara, K. & Akagawa, T., Comparative studies on periodontal tissues around new type artificial roots made of zirconium oxide, titanium and hydroxyapatite. *Phosphorous Res. Bull.*, **1** (1991) 179–84.
8. Nishihara, K., Studies on peri-implantium tissue formation around new type artificial root made of dense hydroxyapatite. *Clin. Mater.*, **12** (1993) 157–67.
9. Nishihara, K. & Nakagiri, S., Studies on stress distribution around hydroxyapatite new type artificial root by means of finite element method. *J. J. S. Biomat.*, **10**(4) (1992) 182–92.
10. Kawahara, H., Tanaka, K., *et al.*, Endosseous implant having polycapillary structure. *US Patent* No. 4964801, October 23, 1990.
11. Wolff, J., Ueber die innere Architectur der Knochen und ihre Bedeutung fur die Frage vom Knochenwachsthum. *Archiv fur pathologische Anatomie Virchovs Archiv.*, **5** (1870) 389–453.
12. Wolff, J., Ueber die Theorie des Knochenschwundes durch vermehrten Druck und der Knochenanbildung durch Druckentlastung. *Archiv fur Klin Chirurgie*, **42** (1891) 302–24.
13. Huiskes, R., Weinans, H., *et al.* Adaptive bone-remodelling theory applied to prosthetic-design analysis. *J. Biomech.*, **20**(11,12) (1987) 1135–50.
14. Meyer, H., Die Architectur der Spongiosa. *Reichert und Dubois-Reymond's Archiv* (1867) pp. 616–28.
15. Fyhrie, D. P. & Carter, D. R., A unifying principle relating stress to trabecular bond morphology. *J. Orthopaedic Res.*, **4** (1986) 304–17.
16. Koch, J. C., The law of bone architecture. *Am. J. Anat.*, **12** (1917) 177–298.
17. Cowin, S. C., Wolff's law of trabecular architecture at remodelling equilibrium. *J. Biomech. Engng*, **108** (1986) 83–8.
18. Gallagher, R. H., Simon, B. R., Joson, T. C. & Gross, J. F., In *Finite Elements in Biomechancis*. John Wiley and Sons, UK, 1982, p. 225.
19. Brunski, J. B., Moccia, A. F. Jr, Pollack, S. R., Korostoff, E. & Trachtenberg, D. I., The influence of functional use of endosseous dental implants on the tissue-implant interface 1 Histological aspects. *J. Dent. Res.*, **58** (1979) 1553–969.